Renewable Energy 119 (2018) 504–512

Contents lists available at ScienceDirect

Renewable Energy

journal homepage: www.elsevier.com/locate/renene

# Single-point reactive power control method on voltage rise mitigation in residential networks with high PV penetration

Maryam Hasheminamin [a], Vassilios Georgios Agelidis [b], Abdollah Ahmadi [a, *], Pierluigi Siano [c], Remus Teodorescu [d]

[a] School of Electrical Engineering and Telecommunications, The University of New South Wales, Sydney, Australia
[b] Department of Electrical Engineering, Technical University of Denmark, 2800 Kgs, Lyngby, Denmark
[c] Department of Industrial Engineering, University of Salerno, Fisciano, Italy
[d] Department of Energy Technology, Aalborg University, Aalborg, 9000, Denmark

A R T I C L E I N F O

*Article history:*

*Keywords:*
Inverter Control
Active and reactive Control
Feeder voltage rise
Photovoltaic
Cost
Droop Control

A B S T R A C T

Voltage rise (VR) due to reverse power flow is an important obstacle for high integration of Photovoltaic (PV) into residential networks. This paper introduces and elaborates a novel methodology of an index-based single-point-reactive power-control (SPRPC) methodology to mitigate voltage rise by absorbing adequate reactive power from one selected point. The proposed index utilizes short circuit analysis to select the best point to apply this Volt/Var control method. SPRPC is supported technically and financially by distribution network operator that makes it cost effective, simple and efficient to eliminate VR in the affected network. With SPRPC none of the previous PV inverters need to upgrade and can retain their unity power factor to not to conflict with current grid codes. Comprehensive 24-h simulation studies are done on a modified IEEE 69-bus Network emulating a traditional residential power system with high r/x ratio. Efficacy, effectiveness and cost study of SPRPC is compared to droop control to evaluate its advantages.



## 1. Introduction

PV sources are increasingly popular in residential networks driven by dual benefits of PV-customers' and distribution network operator (DNO). DNO's motivating policies towards PV customers makes household electricity cost much lower than coal-based electricity price. As was predicted in Ref. [1], the PV generation in Australia is expected to increase from 320 to 1130 MW/year which means total roof top low voltage (LV) PV generated electricity will increase from 16% to 20% by 2031. Under the premise of this exponential uptake of PV penetration in LV network, DNO must assure that the quality of the provided service to PV customers will not be compromised.

PV integration increase in LV network results in reverse power flow (RPF) that would conflict with the promised quality given to customers [2–4]. According to grid codes, ANSI standard C84.1 [5], EN50160 [6] and IEC61727 [7], the voltage DN nodes must remain within 0.95 and 1.05 pu and missing this criterion would disconnect PV-inverter to serve network protection. Hence, voltage rise (VR) would be a major obstacle for increasing PV penetration into existing LV traditional radial networks which were not designed to handle large amount of RPF towards the source [8,9].

Several alleviative methods have been applied to mitigate VR in distribution network (DN) and were evaluated and categorized into two; PV-inverter side and DNO-side approaches in Ref. [2]. Methods such as active power curtailment (APC), buffering excess active power (BEAP) and reactive power control (RPC) which require modification in inverter technologies are listed in Inverter-side approaches, while under load tap changer (ULTC), reconductoring, active grid voltage control (AGVC) and optimal energy management (OEM) are named as DNO-side approaches.

Although, BEAP prevent the surplus active power curtailment by storing it, and despite the numerous advantages [10], is not employed by residential PV-customers due to high cost. Traditionally, DNOs can reduce the secondary voltage of the upstream transformer by applying ULTC. The inability of the ULTC to change frequently and the induced stress, are the main drawbacks of such method [11–13]. Moreover, it also requires communication

* Corresponding author.
*E-mail addresses:* ahmadi.abdollah.janah@gmail.com, a.ahmadi@student.unsw.edu.au (A. Ahmadi).

https://doi.org/10.1016/j.renene.2017.12.029

between the meters and control centre including a transformer, to maintain the feeder voltage within limits [14]. Alternatively, DNO could choose to reinforce the LV network conductor sizes, namely re-conductoring, to reach lower resistance in feeder line. Such practice was applied in some countries because PV penetration increased much faster than inverter development or grid code update, although it has imposed massive costs [15]. In Refs. [16–18] OEM framework was proposed to fulfill the voltage criteria and avoid VR in LV network. Alternative ideas such as [19,20], introduced real-time control to schedule the inverters' active and reactive power which in current state of most LV networks, such methods are less feasible and more expensive considering the required advanced mathematical analysis, dependency on data infrastructure and difficulty of implementation [21–23].

Accordingly, since the mutual benefit of DNO and PV customers, correlates directly to the amount of PV's RPF during the day, APC approaches should also rarely be practiced [23–27]. RPC is recognized as a more viable option for mitigating VR, applied based on droop control [8,28–30]. RPC imposes cost and complexity, and it necessitates to upgrade PV-inverters. Otherwise, they can limit the active power feed-in of PV-inverters, resulting in loss of PV customer revenue [31–34].

According to grid codes such as IEEE standard 1547, PV-inverters are prohibited to interfere with voltage regulation. Although, deliberations are under progress to relieve such constraint and allow individual PVs to contribute in voltage control. Additionally, the major concern of a DNO in high PV integration is to maintain highest possible hosting capacity (HC) for each PV-inverter in sunny hours of the day. It is also, DNO's responsibility to maintain networks' voltage level within grid code criteria. As mentioned earlier, in residential DN, PV-inverters normally do not install storages, and consequently, they would lose revenue of if their inverter switches off due to VR. Consequently, in this paper, a novel methodology is proposed that employ only one PV inverter, and reactive power is suggested to be absorbed centrally. This method is named single point reactive power control (SPRPC), which is an index-based analytic solution for eliminating the VR caused by RPF in a residential DN. By SPRPC short circuit analysis and feeder impedance are utilized to select one PV node through an impedance-voltage rise index (IVRI). The required reactive power to be absorbed is also estimated upon a proposed algorithm to determine the rating of the selected PV-inverter. Considering that, if a PV inverter tends to absorb significant level of reactive power, it is necessary to coordinate a charging mechanism with the DNO to cover the costs associated with extra inverter size and transmitting the additional reactive power, SPRPC is a DNO side approach and would be supported by DNO, technically and financially.

To the knowledge of the authors, this is the first time that literature has managed to employ an index-based RPC methodology from DNO side considering feeder impedance. Previous studies on this topic are extended in the following ways: 1) Technically this method does not breach grid code of voltage regulation and controlling coordination concerns are respected by DNO. 2) Owing to the central fashion of SPRPC, none of the pre-installed PV inverters must be replaced by higher rating inverter which imposes extra costs and hassles to PV-customers. 3) SPRPC mitigates VR to a very acceptable extent in the modified IEEE 69-bus network that cancels or defers the need for DN conductor reinforcement by DNO. 4) Considering that, sunny hours of the days are the times that reactive power capability is most needed and inverter capacity might be occupied mostly by the generated active power of the PV itself, the required reactive power capability of the selected PV-inverter has estimated accurately through a mathematical algorithm which is significantly important. 5) The power losses and transmitting power requirement of SPRPC is less than droop control. 6) According to presented cost study, the associated cost of SPRPC is less than droop. 7) The real verisimilitude models for residential loads and insolation of Sydney, Australia are considered. 8) The study is performed by a powerful DIgSILENT power factory simulator. This enabled the authors to utilize the network effect of the DN in VR mitigation, which mostly neglected in the previous literature. The main purpose of this analysis is to prove that SPRPC, can capably eliminate VR, at essentially no extra cost to the consumer. Comprehensive simulation studies are presented to support its effectiveness.

The remainder of the paper is organized as follows: Section 2 provides a mathematical analysis of the proposed methodology. The test network is introduced, and results of SPRPC are illustrated and compared to droop control in Section 3. Section 4 presents cost study of SPRPC and droop control. Finally, SPRPC methodology is discussed and evaluated in Sections 5 and 6 respectively, where concluding remarks are provided.

## 2. Analytical SPRPC formulation

The proposed methodology is performed in two analytical steps as follow:

### 2.1. Mathematical analysis RPC application to VR mitigation due to RPF

Fig. 1 (a) shows a typical pair of distribution nodes with domestic loads, $P_{dl}$ and $Q_{dl}$, and rooftop grid-connected PV generators to analyse the RPF and the VR phenomenon. The parameters $P_m$ and $Q_m$ represent the net active and reactive power, respectively, at a typical node m which can be determined by Eq. (1). $P_r$ and $Q_r$ are the transmitted active and reactive power between nodes m and n, respectively presented in Eq. (1) which are load nodes in load flow calculations. Vectors depicted in Fig. 1(b), illustrate how voltage $U_m$ raises due to the injected current $I_r$. Eq. (2) shows load flow major equations that calculates above parameters, where $G_{mn}$ is the real part and $B_{mn}$ is the imaginary part of the element in the bus admittance matrix $Y_{BUS}$ corresponding to the nodes m and n. $\delta_{mn}$ is the difference in voltage angle between nodes m and n and the Jacobian matrix (J) represents the partial derivatives of the active

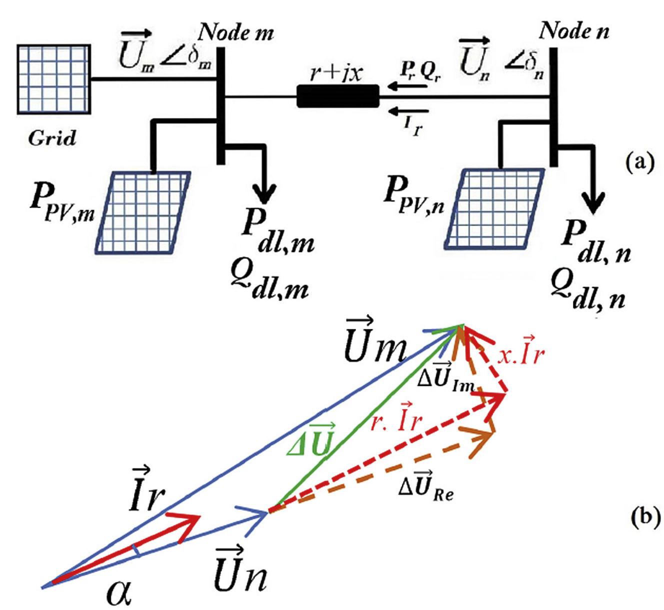


**Fig. 1.** Voltage vectors of 2 adjacent nodes, m, and n in a DN.

and reactive powers with respect to a change in voltage $\Delta U$ and phase angle $\Delta\delta$ and $\vec{U}_m$ is the voltage at node m.

For power systems, a strong coupling is normally observed between P and δ, as well as between Q, and U. This property is employed in the next Jacobian matrix to simplify the computations. In the steady state time window of this research changes in δ of each bus and the coupled P is not taken into consideration and reactive power Q relates to the bus voltage U. Therefore, following linear approximation, Eq. (5) applies to Eq. (3) moreover, (4) which results in Eqs. (6) and (7). Notably, VR may occur not only at the end nodes but also at any point along the feeder. It also can be detected in an adjacent node. The matrix of Eq. (8) shows the correlation of reactive power, Q(U) and bus voltages to each other and points out how network effect can be employed in VR mitigation.

$$\begin{aligned} P_m &= \sum_{n=1}^{N} |\vec{U}_m||\vec{U}_n|(G_{mn}\cos(\delta_{mn}) + B_{mn}\sin(\delta_{mn})) \\ Q_m &= \sum_{n=1}^{N} |\vec{U}_m||\vec{U}_n|(G_{mn}\sin(\delta_{mn}) - B_{mn}\cos(\delta_{mn})) \end{aligned} \tag{1}$$

$$\begin{bmatrix} \Delta P_m \\ \Delta Q_m \end{bmatrix} = \begin{bmatrix} J_{P\delta} & J_{PU} \\ J_{Q\delta} & J_{QU} \end{bmatrix} \begin{bmatrix} \Delta\delta \\ \Delta U \end{bmatrix} \tag{2}$$

$$[\Delta P_m] = [J_{P\delta}][\Delta\delta] + [J_{PU}][\Delta U] \tag{3}$$

$$[\Delta Q_m] = [J_{Q\delta}][\Delta\delta] + [J_{QU}][\Delta U] \tag{4}$$

$$[J_{PU}] \cong 0,\ [J_{Q\delta}] \cong 0 \tag{5}$$

Accordingly, Eqs. (6) and (7) are derived.

$$[\Delta P_m] = [J_{P\delta}][\Delta\delta] \tag{6}$$

$$[\Delta Q_m] = [J_{Q\delta}][\Delta\delta] \tag{7}$$

$$\left[\frac{\Delta U}{\Delta Q}\right] = \begin{bmatrix} \frac{\Delta U_2}{\Delta Q_2} & \frac{\Delta U_2}{\Delta Q_3} & \cdot & \cdot & \frac{\Delta U_2}{\Delta Q_m} \\ \frac{\Delta U_3}{\Delta Q_2} & \frac{\Delta U_3}{\Delta Q_3} & \cdot & \cdot & \frac{\Delta U_3}{\Delta Q_m} \\ \cdot & \cdot & \cdot & \cdot & \\ \cdot & \cdot & \cdot & \cdot & \\ \frac{\Delta U_m}{\Delta Q_2} & \frac{\Delta U_m}{\Delta Q_3} & \cdot & \cdot & \frac{\Delta U_m}{\Delta Q_m} \end{bmatrix} \tag{8}$$

To understand and control VR due to RPF, mathematical analysis is necessary. PV-inverter is designed to become disconnected by the coupled relay if of (8), exceeds set limits. $\Delta\vec{U}$ consists of real and imaginary components, $\Delta\vec{U}_{\mathrm{Re}}$ and $\Delta\vec{U}_{\mathrm{Im}}$ as given in Eq. (9). r and x are the total real and imaginary parts of interconnecting line impedance r + jx, respectively, and $\alpha$ is the phase shift between $\vec{U}_n$ and $\vec{I}_r$, which is the reverse injected current towards the grid depicted on Fig. 1(b).

$$\Delta\vec{U} = \vec{U}_m - \vec{U}_n = \Delta\vec{U}_{\mathrm{Re}} + \Delta\vec{U}_{\mathrm{Im}} \tag{9}$$

$$\begin{aligned} |\Delta\vec{U}_{\mathrm{Re}}| &= r|\vec{I}_r|\cos\alpha - x|\vec{I}_r|\sin\alpha \\ |\Delta\vec{U}_{\mathrm{Im}}| &= x|\vec{I}_r|\cos\alpha + x|\vec{I}_r|\sin\alpha \end{aligned} \tag{10}$$

By substituting the equivalent of active and reactive power in (8) and (9), Eqs. (10) and (11) are derived for $\Delta\vec{U}$:

$$\begin{aligned} |\Delta\vec{U}_{\mathrm{Re}}| &= \frac{r\,P_r - x\,Q_r}{|\vec{U}_m|} \\ |\Delta\vec{U}_{\mathrm{Im}}| &= \frac{x\,P_r + r\,Q_r}{|\vec{U}_m|} \end{aligned} \tag{11}$$

$$|\Delta\vec{U}| = \frac{r\,P_r - x\,Q_r}{|\vec{U}_m|} + \frac{x\,P_r + r\,Q_r}{|\vec{U}_m|} \tag{12}$$

Therefore, the amount of voltage deviation depends on r, x, $P_r$ and $Q_r$ and it increases when $I_r$ reverses from m to n. Eq. (12) presents the power relations, where $Q_\gamma$ is the amount of reactive power to be absorbed by the PV inverter to eliminate VR and regulate the voltage back to its nominal value. Accordingly, Eq. (13) can be written, considering these relations and can be ordered to (14) by considering the absolute value of vectors. It comprises of $U_m$, $U_n$, PV and inverter powers as shown. Eq. (14) can be rearranged to (15) as a quadratic equation.

$$\begin{cases} P_r = P_{pv,m} - P_{dl,m} \\ Q_r = Q_{pv,m} - Q_{dl,m} \\ Q_s = Q_r + Q_\gamma \end{cases} \tag{13}$$

$$\begin{aligned} \vec{U}_m^2 = &\left[\vec{U}_n + \frac{r(P_{pv,m} - P_{dl,m}) + x(Q_r + Q_\gamma)}{|\vec{U}_m|}\right]^2 \\ &+ \left[\frac{x(P_{pv,m} - P_{dl,m}) - r(Q_r + Q_\gamma)}{|\vec{U}_m|}\right]^2 \end{aligned} \tag{14}$$

$$\begin{aligned} &U_n^4 + 2U_n^2\left[r(P_{pv,m} - P_{dl,m}) + x(Q_r + Q_\gamma) - \frac{U_m^2}{2}\right] \\ &+ \left(r^2 + x^2\right)\left[(P_{pv,m} - P_{dl,m})^2 + (Q_r + Q_\gamma)^2\right. \\ &= 0 \end{aligned} \tag{15}$$

$$U_n^4 + 2U_n^2\left[(r\,P_r + x\,Q_s) - \frac{U_m^2}{2}\right] + \left(r^2 + x^2\right)\left[\left(P_r^2 + Q_s^2\right] = 0 \tag{16}$$

$$\begin{aligned} \Gamma &= \sqrt{\frac{U_m^4}{4} + U_m^2[r\,P_r + x\,Q_s] - [xP_r - rQ_s]^2} \\ U_n &= \sqrt{\frac{U_m^2}{2} - [r\,P_r + x\,Q_s] + \Gamma} \end{aligned} \tag{17}$$

Eq. (16) must be solved for $Q_s$ where K in the permitted ratio of over voltage according to grid codes:

$$\begin{aligned} &AQ_s^2 + BQ_s + C = 0 \\ &\begin{cases} A = \left(x^2 + r^2\right) \\ B = 2xU_mU_n \\ C = \left[P_r^2\left(x^2 + r^2\right)\right] + [2rU_nU_mP_r] + \left[U_m^2U_n^2 - U_m^4\right] \end{cases} \end{aligned} \tag{18}$$

$$U_m = kU_n \tag{19}$$

$$\left(x^2+r^2\right)Q_s^2+\left(2xKU_n^2\right)Q_s+\left(\left[P_r^2\left(x^2+r^2\right)\right]+\left[2rP_rKU_n^2\right]+\left[\times\left(K^2U_n^4-K^4U_n^4\right]\right)=0 \tag{20}$$

$$\Delta=\left[2xKU_n^2\right]^2-4\left(x^2+r^2\right)\left[P_r^2\left(x^2+r^2\right)\right]+\left[2rP_rKU_n^2\right]+\left[K^2U_n^4-K^4U_n^4\right] \tag{21}$$

$$Q_s=\frac{-(2xKU_n)+\sqrt{\Delta}}{2\left(x^2+r^2\right)} \tag{22}$$

$$K=1.05$$

$$S_{pv,m}=\sqrt{P_{pv,m}^2+Q_{pv,m}^2} \tag{23}$$

$$\xi=\frac{S_{pv,m}}{P_{pv,m}} \tag{24}$$

$$\gamma=\sqrt{\zeta^2-1} \tag{25}$$

$$Q_{pv,m}=Q_{\gamma,m}=P_{pv,m}\gamma \tag{26}$$

$$\frac{P_r-jQ_r}{U_n\angle\delta_n}=\frac{U_m\angle\delta_m-U_n\angle\delta_n}{r+jx} \tag{27}$$

$$\delta_m=\alpha,\delta_n=0 \tag{28}$$

$$\Rightarrow\begin{cases}R_{sc}P_r+X_{sc}Q_r=-U_n^2+U_nU_m\cos\alpha\\ X_{sc}P_r-R_{sc}Q_r=U_nU_m\sin\alpha\end{cases} \tag{29}$$

$$\Rightarrow\begin{cases}\left(R_{sc}^2+X_{sc}^2\right)P_r=\\ -R_{sc}U_n^2+R_{sc}U_nU_m\cos\alpha+xU_nU_m\sin\delta\end{cases} \tag{30}$$

$$\mathrm{P}_r=\frac{KU_n^2}{\left(R_{sc}^2+X_{sc}^2\right)}\left[\frac{-R_{sc}}{K}+(R_{sc}cos\alpha)+X_{sc}sin\alpha)\right] \tag{31}$$

$$\frac{\partial P_r}{\partial\alpha}=\frac{KU_n^2}{\left(R_{sc}^2+X_{sc}^2\right)}[R_{sc}sin\alpha-X_{sc}\cos\alpha]=0 \tag{32}$$

$$\tan\alpha=\frac{X_{sc}}{R_{sc}} \tag{33}$$

$$\frac{P_{pv,m}}{P_{r,HC}}=IVRI \tag{34}$$

Eqs. (1)–(26) elaborate the reactive power compensation method for voltage rise mitigation, mathematically. They show that voltage deviation depends on the r and x of feeder even in DN which r/x ration is relatively high. The methodology estimates the adequate $Q_s$ to compensate the unwanted raise in voltage by absorbing amount of reactive power. Hence the $U_m$ can be equal to $U_n$ or up to K times greater such as 1.05, reflecting the 5% permitted VR by grid. Fig. 2 illustrates the mechanism on the feeder and in vectors. $\beta$ is the angle of the shifted current that results in a new voltage deviation, $\Delta\vec{U}$.

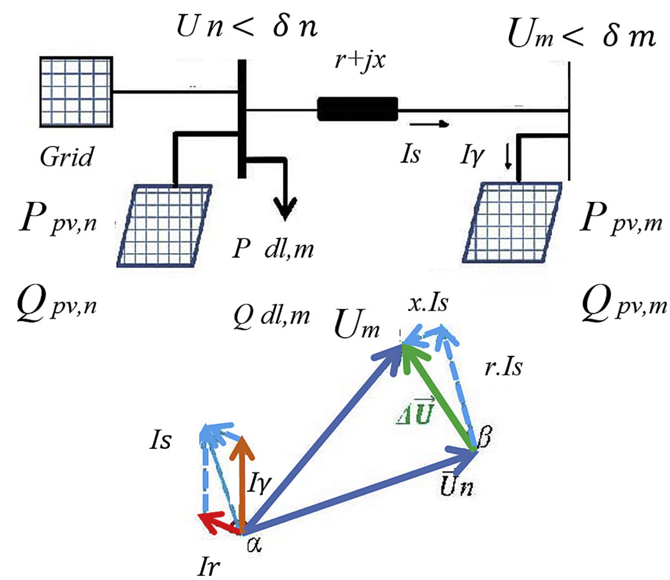


**Fig. 2.** Controlled voltage vectors of 2 adjacent nodes, m and n in a DN.

In PV-inverters with no extra reactive power rating, when PV active power generation is at its maximum, the reactive power is minimum ($Q_{pv,m}$ - min) whereas the maximum PV reactive power ($Q_{pv,m}$ - max) is obtained using the total inverter capacity when PV active power production is zero. In order to apply the RPC and injecting/absorbing reactive power at peak active power generation, the rating of PV-inverters must upgrade with higher reactive power capability. Accordingly, the PV node should be able to absorb adequate amount to be able to absorb adequate amount of $Q_s$. Therefore, $Q_s$ must cover both reactive part of the load, $Q_r$ as well as $Q_\gamma$. Eqs. (26) and (27) which is specifically for voltage regulation. These are presented on Fig. 2 by $\vec{I}_\gamma$ and $\vec{I}_s$.

The rating factor $\xi$ is defined as the reactive power coefficient. By multiplying $\xi$ by the maximum PV active power generation, $P_{pv,m}$-max, the apparent power of the inverter is determined. $\xi$ can vary between 0 and any 'user defined value'. A Higher value of $\xi$ provides better voltage control capability, although imposes an extra cost. Hence there is a trade-off between more costly inverters and their voltage control benefits which is an important concern of DNO.

### 2.2. SPRPC and IVRI methodology

A review of the relevant literature failed to find any studies considering DNO applying central reactive power control to mitigate VR. Previous studies have focused on developing inverter-control technologies that involve PV customers. Most of PV customers, if not all of them, do not have storages and their inverters are feeding their domestic active load. Applying RPC to all PV customers involves them with inverter upgrading, control complexity, and relevant imposed costs. Considering that PV-customers are not entitled to regulate voltage, they may not tend to pay the extra cost, while they seek their revenue from rooftop PVs to trade the PV power that they inject into the grid. Therefore, DNO is responsible to regulate voltage and avoid VR to be able to increase HC and let more PV energy to get into the grid.

This paper suggests a smart novel comprehensive methodology that attempts VR mitigation by a central reactive power control approach, namely SPRPC. SPRPC benefits from the network effect, presented by Eq. (8), to eliminate VR with less cost and more

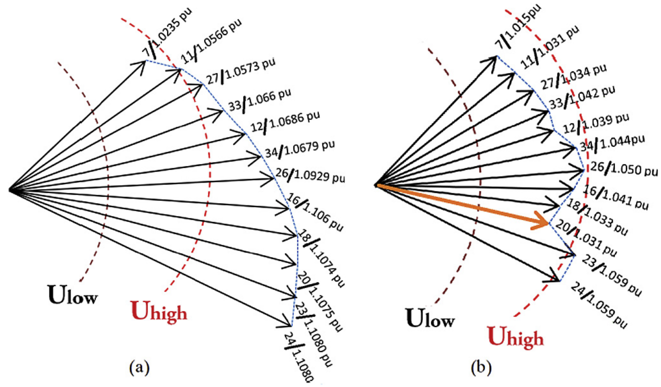


**Fig. 3.** Each vector is labeled by Node number, Voltage [pu], (a) Random voltage vectors before SPRPC(B)Random voltage vectors after SPRPC.

simplicity, while serves broader part of the network by engaging only one node. In this regard, the most effective point of the network, in the sense of voltage sensitivity must be recognized. Accordingly, an impedance-voltage rise index (IVRI) is defined in Eq. (34) that considers the short circuit impedance of the connecting feeder and its effect on voltage performance to help with best node selection. Fig. 3 schemes random voltage vectors before and after SPRPC application.

IVRI computes the maximum HC and compares it to the PV generated power, while the VR criteria up to 1.05 pu is satisfied at each node. Feeder impedance is considered in IVIR calculations which increases the accuracy of HC concept, defined in the previous literature. Eq. (27) defines the balanced equation at each node where Pr is the injected PV power into the grid. $R_{sc}$ and $X_{sc}$ are the short circuit impedance between node m and source n. Eq. (28) is assumed for $\delta_m$ and $\delta_n$. Hence, for extracting $P_r$ out of Eq. (28), $Q_r$ must be removed which will results into Eq. (29). $U_m = U_n = K$ and $K = 1.05$ as explained above. Consequently, the maximum value of $P_r$ namely, $P_{r,HC}$ is achieved through Eqs. (30)–(32) for $\alpha$ which results in Eq. (33). Concluding that $\alpha$ is equal to δ. $P_{r,HC}$ leads the study to assess most power sensitive node of the grid via IV RI, defined in Eq. (34).

As it is depicted in the IV RI profile in Fig. 4, node 20 is selected as the most effective node in the modified IEEE 96-bus DN which is subject to SPRPC best node selection.

Flowchart of Fig. 5 presents steps 1–3 of SPRPC methodology.

SPRPC utilizes the time-varying load profile for residential customers of Sydney and the PV generation models over a 24-h time frame for Sydney insolation profile refer to [28]. The

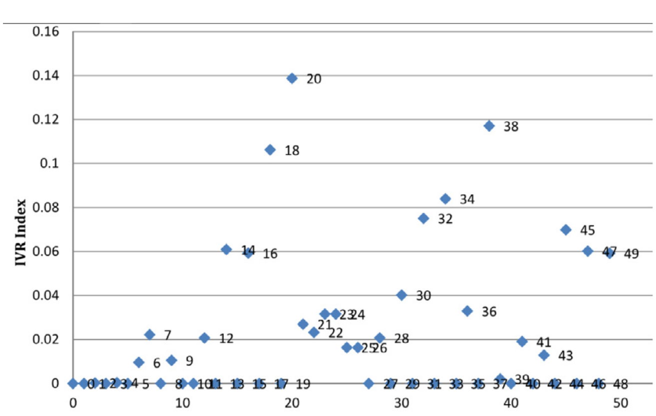


**Fig. 4.** IVRI profile for modified 69-bus DN.

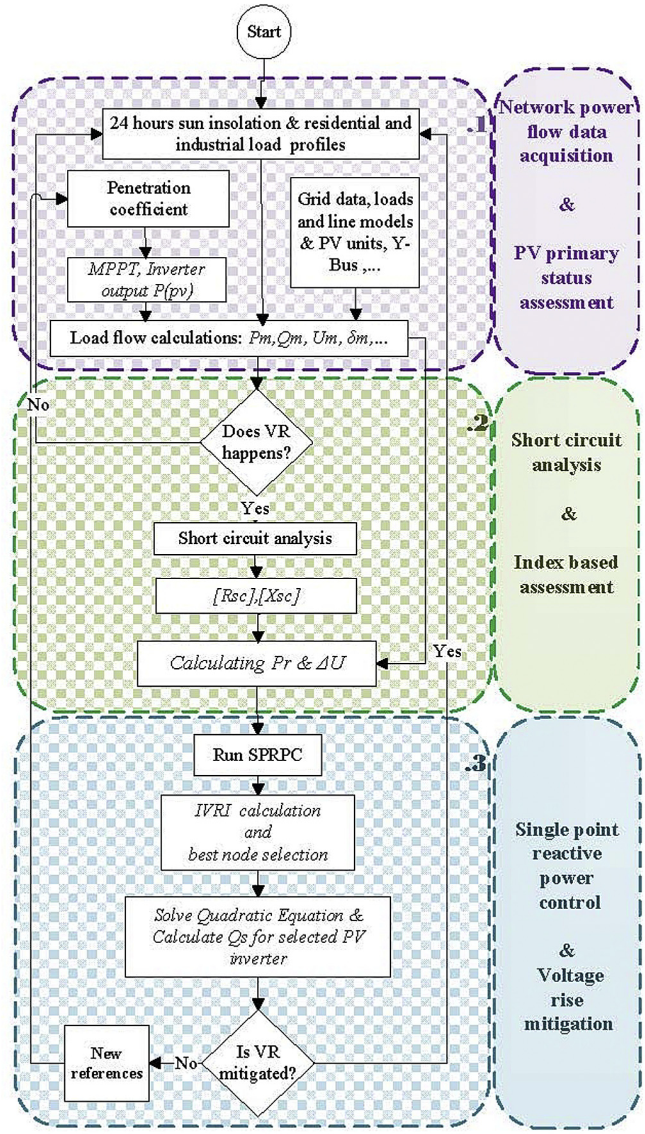


**Fig. 5.** Flowchart of mitigation.

flowchart shows that after assessing the DN and data acquisition from the load, flow is step 1 the DN is assessed for VR. The short circuit analysis was also run in step 2 to extract relevant impedances of the network. $P_r$, equal to PBI and $\Delta U$ are calculated for general voltage assessment accordingly. In step 3, $Q_s$ values are calculated for each node which feeds the droop control method. For SPRPC, the flowchart can lead to step 4 as a shortcut and the IV RI profile is extracted to pinpoint the single control node of DN.

The amount of $\gamma$ required for VR mitigation by PV-inverter is then estimated. Details of this methodology and implemented steps are discussed in section 3.

## 3. VR mitigation scenario and results

VR mitigation methods are applied, elaborated and analysed below on the modified IEEE 69-bus distribution network of Fig. 6 emulating a weak LV residential network. The base case is simulated primarily as a benchmark, and numerical results are obtained.

A- Base case, $\cos\phi = 1$

B- Droop control.

C- IVRI-based SPRPC.

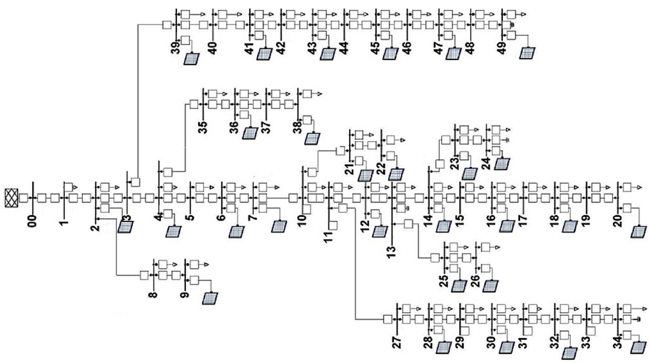

Fig. 6. Modified IEEE 69-bus network.

### 3.1. Base case, cos $\phi = 1$

In most if not all, traditional distribution networks, solar PV inverters operate at unity power factor, and therefore the reactive power capability is zero. Hence, the whole capacity of the inverter is used for real power generation, unless at night which PV generation is zero. Fig. 7 depicts the 24-h voltage profile of all network nodes. The simulation was done for 24 h at 1-h intervals. In this case, PV units are not connected with high penetration. As can be seen in Fig. 8, RPF occurs during the period 3–7 pm and the voltages of several nodes increase above 1.05 pu while P; [0; Ppv,max] and Q; [0] ranges.

### 3.2. Droop control

Voltage droop control works by manipulating the PV reactive power within its reactive power capability while the PV active power remains between zero and $P_{pv,m\text{-}max}$ and the bus voltage is controlled for VR. The amount of reactive power absorption in VR mitigation depends on the voltage reference and the rating of the PV inverter. Exceeding these limits is equivalent to the loss of voltage control. Consequently, the inverter operates in all four quadrants, assuming that reactive power would be injected/absorbed at some points when droop control is active. Droop control for VR seems to be effective as presented in Fig. 9 where specified droop characteristic is applied. However, if the reactive demand at each bus is higher than the remaining capacity of the inverter, then $Q_{pv,m\text{-}max} = Q_{set,m}$ where $Q_{set,m}$ is the rated reactive power for PV inverter. Accurate estimation of the reactive power capability of the inverter becomes critical for making the system more efficient. By applying the above droop control method to each inverter with $\gamma = 1.2$, the 24-h voltage profile of Fig. 9 is achieved. As can be seen in this figure, VR is significantly reduced, except for a number of highly sensitive nodes which still experience VR at particular times of the day. Fig. 10 depicts the percentage of PV-inverters' loading to achieve the regulated voltage regulation in Fig. 9. Accordingly, Fig. 11 illustrates the amount of reactive power, each inverter absorb/inject in different hours of a day. Finally, Fig. 12 depicts a 3D view of reactive power profile vs. time for each PV-inverter.

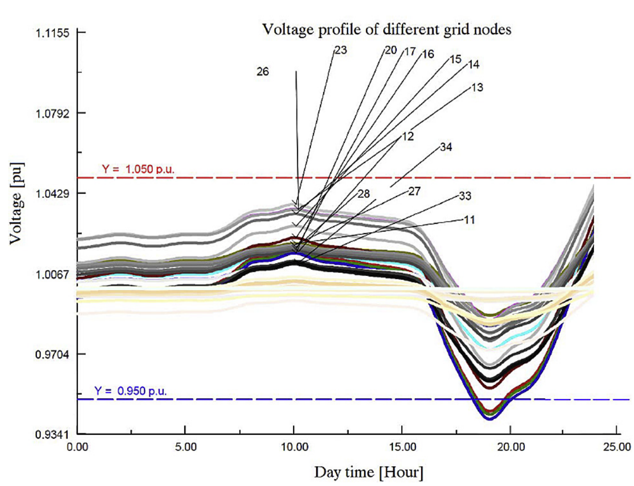


Fig. 7. 24-h Voltage profile of all grid nodes without PVs in service is the modified DN.

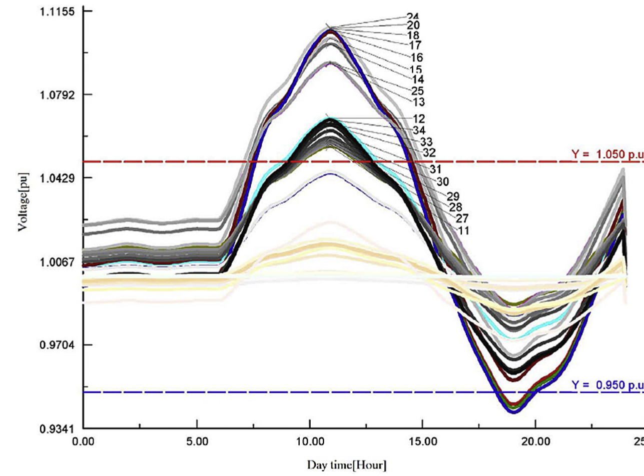


Fig. 8. 24-hour voltage performance assessment with PV units at unity power factor.

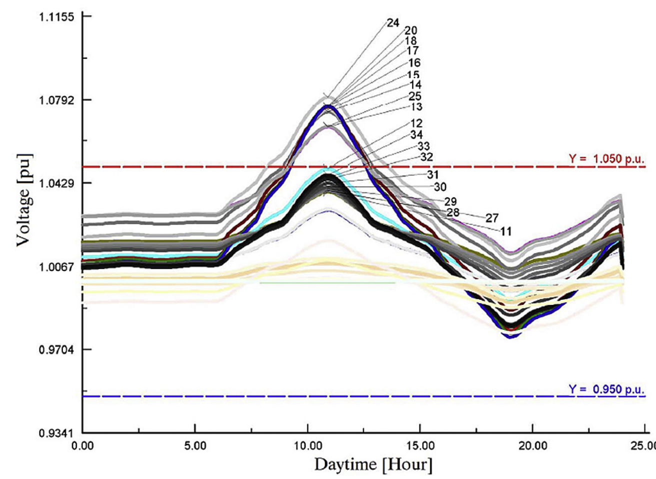


Fig. 9. 24 h voltage profile controlled by Q(V)characteristic (droop).

### 3.3. IVRI-based SPRPC

It must be considered that the effect of RPF on VR varies, depending on the line impedance, inverter loading and reactive power capability. Development of indices is therefore beneficial for analysing and comparing the impact of impedance on VR for different feeders in a DN with varying load and insolation conditions. Eqs. (28)–(34) elaborate the definition of the index IV RI and the result of the assessment identifies node 20 for having the highest value of IV RI. Single point reactive power control, SPRPC is applied to the same network for evaluation of its efficacy. Fig. 13

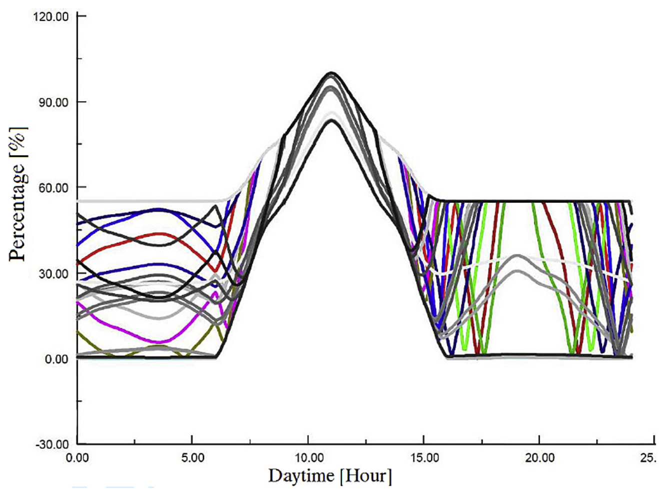


**Fig. 10.** Loading of PV inverters as a function of time with droop control.

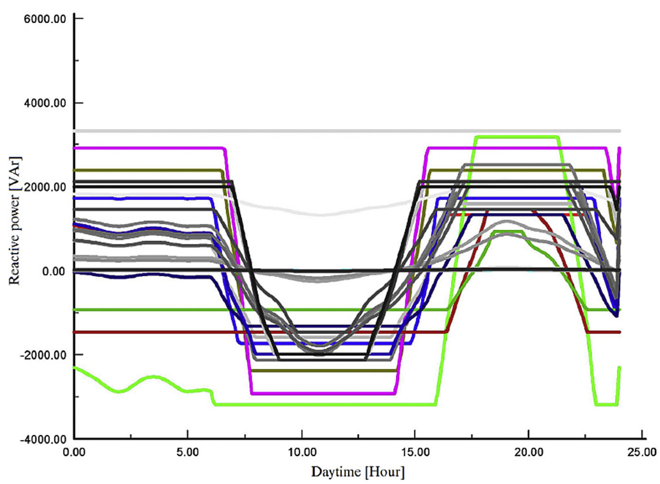


**Fig. 11.** Reactive power of PV systems as a function of time with droop control.

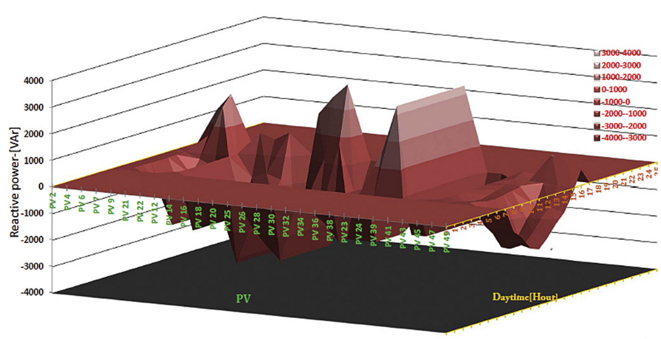


**Fig. 12.** 3D reactive power vs. time for PV inverters with droop control.

shows the resultant 3D reactive power profile vs. time for each PV node, which applies SPRPC on selected node 20 through IVRI assessment.

Fig. 14 shows the 24-h voltage profile for all network nodes, which have been significantly improved after applying the SPRPC method.

## 4. Cost study

Electric PV generation technologies included in current cost study is the total installation, operation and maintenance costs for grid-tied residential, commercial and industrial PV facilities which are estimated. Technologies considered are technically proven and commercially available. The capital and maintenance cost data used in the calculations are from the current SMA distributor in Australia 2013 updated sources. 2012 data was used to supplement the update or when new data was unavailable [35]. The data behind the PV cost estimates were more numerous because it is a widely deployed technology and given as an average. Data for operation and maintenance (O and M) were given similarly as an average. Table 2 presents PV costs in different categories: The data, however, may become out of date as the decreases in the price of modules and inverters over the last few years. The current report documenting current market prices of SMA Australia insight report. The extra cost of PV which is due to reactive power capability is considered in Table 2 [36].

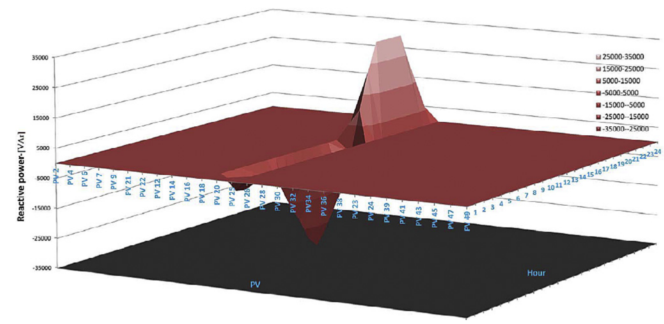


**Fig. 13.** 3D reactive power vs. time for PV inverters with central droop control.

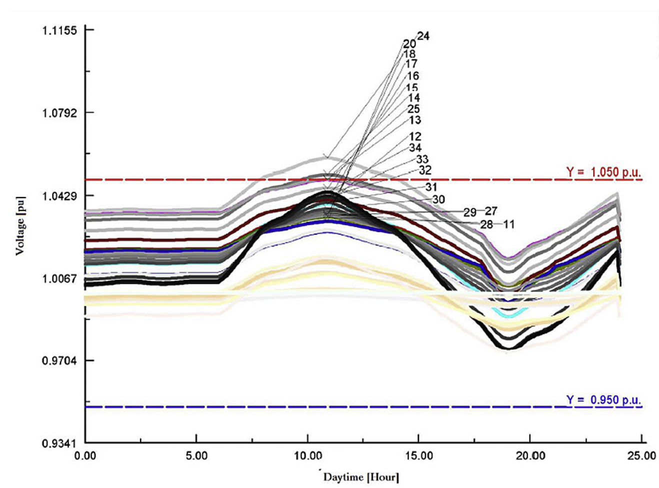


**Fig. 14.** SPRPC strategy with reactive power capability equal to 30 Kvar.

$$t = \eta_{OM}\pi_{OM} + \eta_{Inv}\pi_{Inv} \tag{35}$$

where $\pi_{OM}$ and $\pi_{Inv}$ are the extra reactive power capacity for operation and maintenance and inverter itself, respectively. Similarly, $\eta_{OM}$, and $\eta_{Inv}$ are the relevant cost of the cumulative inverter capacity with droop control or SPRPC for VR mitigation.

## 5. Discussion

In this section, the proposed methodology, SPRPC which was elaborated in previous sections for VR mitigation methods is compared with droop control as the state of the art of RPC methods. Comparing the outcome of droop control in Fig. 9 with the base

**Table 1**
Individual and cumulative calculation of reactive power capability required in droop control method.

| Name | Active Power [W] | Reactive Power [var] | Apparent Power [VA] | Name | Active Power [W] | Reactive Power [var] | Apparent Power [VA] |
|---|---|---|---|---|---|---|---|
| PV 12 | 1714.286 | -1326.65 | 2167.666 | PV 32 | 2571.429 | -1989.975 | 3251.499 |
| PV 14 | 4114.286 | -3183.96 | 5202.399 | PV 36 | 4285.715 | 1392.492 | 4506.261 |
| PV 16 | 2228.572 | -1724.645 | 2817.966 | PV 38 | 4285.715 | 3316.625 | 5419.165 |
| PV 18 | 3085.715 | -2387.97 | 3901.799 | PV 39 | 4285.715 | -17.11062 | 4285.749 |
| PV 2 | 2742.857 | -6.231866 | 2742.865 | PV 4 | 2742.857 | -9.050409 | 2742.872 |
| PV 20 | 3771.43 | -2918.63 | 4768.867 | PV 41 | 2742.857 | -176.5062 | 2748.531 |
| PV 21 | 2742.857 | -2122.64 | 3468.266 | PV 43 | 1714.286 | -121.571 | 1718.591 |
| PV 22 | 2057.143 | -1591.98 | 2601.199 | PV 45 | 3257.143 | -1590.488 | 3624.725 |
| PV 23 | 1885.715 | -1459.316 | 2384.434 | PV 47 | 2742.857 | -1425.012 | 3090.943 |
| PV 24 | 1885.715 | -1459.316 | 2384.434 | PV 49 | 2571.429 | -1576.394 | 3016.167 |
| PV 25 | 1200 | -928.6549 | 1517.366 | PV 6 | 1885.715 | -1459.316 | 2384.434 |
| PV 26 | 1200 | -928.6549 | 1517.366 | PV 7 | 2742.857 | -2122.64 | 3468.266 |
| PV 28 | 1714.286 | -1326.65 | 2167.666 | PV 9 | 1714.286 | -8.659822 | 1714.308 |
| PV 30 | 2571.429 | -1989.975 | 3251.499 | PV34 | 2571.429 | -1989.975 | 3251.499 |

Cumulative reactive power capacity demand 40551.1.

**Table 2**
Cost estimation and PV prices.

| Droop control: | SPRPC: |
|---|---|
| $\Pi OM = 40.551$ [kVAr] | $\Pi OM = 32.2$ [kVAr] |
| $\Pi SPRPC = 0$ [kVAr] | $\Pi SPRPC = 32.2$ [kVAr] |
| $\eta OM = 17.85$ [$/kVA-year] | $\eta OM = 16.15$ [$/kVA-year] |
| $\eta Inv = 450$ [$/kVA- year] | $\eta Inv = 200$ [$/kVA- year] |

case of Fig. 8 in the modified IEEE 69-bus network, shows that the reactive power capability provides effective VR mitigation. Accordingly, SPRPC methodology was presented in Figs. 13 and 14, whereby reactive power is compensated in one selected central point to maintain the desired voltage at a reference value. As can be seen in diagrams and voltage profiles, VR is almost eliminated by SPRPC. Table 1 calculates the cumulative amount of reactive power and shows that much less reactive power capacity was utilized in SPRPC, 32.2 kVAr, while results in highly better performance. The Cost study of Eq. (35) reports 18971 Dollar for droop control and 12880 Dollar for SPRPC with better VR elimination.

The main advantage of SPRPC, apart from the lower cost is that all other PV inverters in the DN network can remain at their unity power factor without any need to inverter upgrading. As it is depicted in Table 1 the inverter rating for the PV system at selected node 20, is only 30 KVA and even less than the cumulative sum of the reactive power absorption of all other PV-inverters in droop control scenario. The cumulative amount of inverters initial rating are even more than their real absorption. The total amount of saved money by SPRPC is 6091 Dollar in the studied scenarios. SPRPC is considered as a DNO-side method, as installing a central compensator in one of the load nodes may not affordable for a residential customer. Furthermore, other network nodes can also benefit, while DNO provides an opportunity to allow more PV generators to penetrate into the network. In other words, the total integration capacity of PV into the network can be effectively increased. Another noteworthy result for the SPRPC method is that the practical topology requires a limited number of switching actions to facilitate its implementation, while all other PV inverters can remain unchanged with unity power factor. SPRPC is an efficient, simple, cost-effective and feasible solution that can be applied to any VR affected DN and enhance the HC while improving the voltage profile of the network during both day and night.

## 6. Conclusion

This paper has dealt with VR owing to RPF in DNs with high PV penetration. The proposed SPRPC method allows the subset of bidirectional PV inverters that strongly impact both the voltage profile and network performance objectives to be identified. The method can also quantify the amount of active and reactive power to be procured from the PV system at the selected node. An Impedance-Voltage Rise Index (IVRI) was used to quantify and minimize the inverter rating required to eliminate VR throughout the distribution feeder. Cost efficiency comparison is also presented to show the economic advantage of SPRPC comparing to droop control strategies. SPRPC does not need any data infrastructure for communicating. All pre-installed PV-inverters retain their unity power factor and rating in the DN. Notably, the SPRPC imposes much less switching practices which makes it simple to implement and does not require communication or cooperation among other PV-inverters.

Unity power factor can be retained for all other PV units on other nodes. Although the formulated SPRPC method requires a significant amount of calculation, it avoids lots of switching and extra calculations for all other PV inverters. The method provides indices by considering distribution network line impedances and short circuit analysis. Real sun insolation and load profiles for New South Wales, Australia, were also considered in calculations. The results show that the SPRPC method significantly reduces VR in the modified IEEE 69-bus network. It does so without compromising inverter ratings and minimises switching within the DN, and without any need for inverter replacement at other nodes.

## References


[1] Australian energy market operator. rooftop pv information paper available on: http://www.aemo.com.au/electricity//media/files/other/forecasting/rooftop pv information paper.ashx, august 2015.
[2] M. Hasheminamin, V. Agelidis, V. Salehi, R. Teodorescu, B. Hredzak, Index-based assessment of voltage rise and reverse power flow phenomena in a distribution feeder under high pv penetration, IEEE J. Photovolt. 99 (2015) 1–11.
[3] P. Da Silva, S. Karnouskos, D. Ilic, Evaluation of the scalability of an energy market for smart grid neighborhoods, in: 11th IEEE International Conference on Industrial Informatics (INDIN), July 2013, pp. 380–385.
[4] R. Mastromauro, M. Liserre, A. Dell'Aquila, Control issues in single-stage photovoltaic systems: Mppt, current and voltage control, IEEE Trans. Ind. Inf. 8 (no. 2) (May 2012) 241–254.
[5] American National Standard for Power Systems and Equipment Voltage Ratings, august 2015 accessed on: https://www.nema.org/standards.
[6] D. Start, A review of the new cenelec standard en 50160, in: IEE Colloquium on Issues in Power Quality, Nov. 1995, 4/1–4/7.
[7] IEEE Recommended Practice for Interconnecting Distributed Resources with Electric Power Systems Distribution Secondary Networks, 2011, pp. 1–38. IEEE Std 1547.6-2011.
[8] T. Stetz, F. Marten, M. Braun, Improved low voltage grid integration of photovoltaic systems in Germany, IEEE Trans. Sust. Energy 4 (no. 2) (April 2013) 534–542.

[9] D.Q. Hung, N. Mithulananthan, K. Lee, Determining pv penetration for distribution systems with time-varying load models, IEEE Trans. Power Syst. 29 (no. 6) (Nov 2014) 3048–3057.
[10] M. Kabir, Y. Mishra, G. Ledwich, Z. Dong, K. Wong, Coordinated control of grid-connected photovoltaic reactive power and battery energy storage systems to improve the voltage profile of a residential distribution feeder, IEEE Trans. Ind. Inf. 10 (no. 2) (May 2014) 967–977.
[11] X. Liu, A. Aichhorn, L. Liu, H. Li, Coordinated control of distributed energy storage system with tap changer transformers for voltage rise mitigation under high photovoltaic penetration, IEEE Trans. Smart Grid 3 (no. 2) (June 2012) 897–906.
[12] S. Liew, G. Strbac, Maximising penetration of wind generation in existing distribution networks, IEE Trans. Gen., Transm. Distrib. 149 (no. 3) (May 2002) 256–262.
[13] R. Echavarria, A. Claudio, M. Cotorogea, Analysis, design, and implementation of a fast on-load tap changing regulator, IEEE Trans. Power Electron. 22 (no. 2) (March 2007) 527–534.
[14] D.E.-F.T. Tonkoski, R. Turcotte, Impact of high pv penetration on voltage profiles in residential neighborhoods, IEEE Trans. Sust. Energy 3 (no. 3) (July 2012) 518–527.
[15] G. Braun, M. Arnold, H. Laukamp, Plugging into the zeitgeist, IEEE Power Energy Mag. 7 (no. 3) (June 2009) 63–76.
[16] E. Dall'Anese, S. Dhople, Johnson, Giannakis, Optimal dispatch of residential photovoltaic inverters under forecasting uncertainties, IEEE J. Photovolt. 5 (no. 1) (Jan 2015) 350–359.
[17] L. Liu, H. Li, Y. Xue, W. Liu, Reactive power compensation and optimization strategy for grid-interactive cascaded photovoltaic systems, IEEE Trans. Power Electron. 30 (no. 1) (Jan 2015) 188–202.
[18] T. Niknam, A. Kavousi-Fard, A. Ostadi, Impact of hydrogen production and thermal energy recovery of pemfcpps on optimal management of renewable microgrids, IEEE Trans. Ind. Inf. 11 (no. 5) (Oct 2015) 1190–1197.
[19] S. Bolognani, S. Zampieri, A distributed control strategy for reactive power compensation in smart microgrids, IEEE Trans. Autom. Control 58 (no. 11) (Nov 2013) 2818–2833.
[20] A. Samadi, R. Eriksson, L. Soder, B. Rawn, J. Boemer, Coordinated active power-dependent voltage regulation in distribution grids with pv systems, IEEE Trans. Power Deliv. 29 (no. 3) (June 2014) 1454–1464.
[21] J. Miret, M. Castilla, A. Camacho, L. Garci anda de Vicu anda, J. Matas, Control scheme for photovoltaic three-phase inverters to minimize peak currents during unbalanced grid-voltage sags, IEEE Trans. Power Electron. 27 (no. 10) (Oct. 2012) 4262–4271.
[22] P. Carvalho, P. Correia, and L. Ferreira, IEEE Trans. on Power Systems.
[23] E. Demirok, K. Casado Andlez, P. Frederiksen, P.T.R. Sera, D. Rodriguez, Local reactive power control methods for overvoltage prevention of distributed solar inverters in low-voltage grids, IEEE J. Photovolt. 1 (no. 2) (Oct. 2011) 174–182.
[24] N. Kakimoto, Q.-Y. Piao, H. Ito, Voltage control of photovoltaic generator in combination with series reactor, IEEE Trans. Sustain. Energy 2 (no. 4) (Oct. 2011) 374–382.
[25] Y. Liu, B. Ge, H. Abu-Rub, F. Peng, An effective control method for quasi-z-source cascade multilevel inverter-based grid-tie single phase photovoltaic power system, IEEE Trans. Ind. Inf. 10 (no. 1) (Feb 2014) 399–407.
[26] Y. Liu, B. Ge, H. Abu-Rub, F.Z. Peng, An effective control method for three-phase quasi-z-source cascaded multilevel inverter based grid-tie photovoltaic power system, Ind. Electron. IEEE Trans. 61 (no. 12) (Dec 2014) 6794–6802.
[27] M. De Cristofaro, G. Di Capua, N. Femia, G. Petrone, G. Spagnuolo, D. Toledo, Models and methods for energy productivity analysis of pv systems, in: IEEE 13th International Conference on Industrial Informatics (INDIN), July 2015, pp. 1153–1158.
[28] M. Kabir, Y. Mishra, G. Ledwich, Z. Dong, K. Wong, Coordinated control of grid-connected photovoltaic reactive power and battery energy storage systems to improve the voltage profile of a residential distribution feeder, IEEE Trans. Ind. Inf. 10 (no. 2) (May 2014) 967–977.
[29] F. Wu, X. Li, F. Feng, H. Gooi, Modified cascaded multilevel gird-connected inverter to enhance european efficiency, Ind. Inf. IEEE Trans. 99 (2015) 1.
[30] F. Kupzog, H. Brunner, W. Pruggler, T. Pfajfar, A. Lugmaier, Dg demonet-concept - a new algorithm for active distribution grid operation facilitating high dg penetration, in: 5th IEEE International Conference on Industrial Informatics, vol. 2, June 2007, pp. 1197–1202.
[31] R. Yan, T. Saha, Investigation of voltage stability for residential customers due to high photovoltaic penetrations, IEEE Trans. Power Syst. 27 (no. 2) (May 2012) 651–662.
[32] R. Tonkoski, L. Lopes, T. El-Fouly, Coordinated active power curtailment of grid connected pv inverters for overvoltage prevention, IEEE Trans. Sust. Energy 2 (no. 2) (Apr. 2011) 139–147.
[33] P. Jahangiri, D. Aliprantis, Distributed volt/var control by pv inverters, IEEE Trans. Power Syst. 28 (no. 3) (Aug 2013) 3429–3439.
[34] S. Soudi, Distribution system planning with distributed generations considering benefits and costs, I.J.Modern Educ. Comput. Sci. (Feb 2013) 45–52.
[35] National renewable energy labratory accessed on: http://www.nrel.gov/analysis,august 2015.
[36] Sma australia accessed on: http://www.sma-australia.com.au/,august 2015.